厚生労働科学研究研究費補助金

感覚器障害研究事業

網膜血管新生抑制機構の解明とその応用に関する研究

平成１６年度～１８年度　総合研究報告書

主任研究者　細谷　健一

平成１９（２００７）年　３月

目　次

厚生労働科学研究費補助金（感覚器障害研究事業）
（総合）研究報告書

網膜血管新生抑制機構の解明とその応用に関する研究

主任研究者　細谷　健一　富山大学・大学院医学薬学研究部　教授

研究要旨：本研究は、網膜ペリサイトから分泌される網膜血管内皮細胞増殖抑制因子を同定し、網膜血管新生抑制機構を解明することを目的とした。抗中和抗体を用いた解析および遺伝子発現解析から網膜ペリサイト由来液性因子による網膜血管内皮細胞増殖抑制効果において、過去に報告されている TGF-βの関与は一部であることが示された。網膜ペリサイト培養液で処理した網膜血管内皮細胞の GeneChip 解析から、growth arrest DNA damage-inducible 45 gene など血管新生や細胞増殖抑制に関わっていると考えられる遺伝子候補を多数同定した。網膜ペリサイト由来の新規血管内皮細胞増殖抑制液性因子としてトロポミオシンの新規アイソフォームを単離、同遺伝子のクローニングに成功し、リコンビナントタンパク質を作製、網膜血管内皮細胞の増殖抑制活性を証明した。新規トロポミオシンは 50%阻害濃度（IC_{50}）約 2 μM で、網膜血管内皮細胞の増殖を抑制した。さらに、網膜ペリサイト由来の血管内皮細胞増殖抑制液性因子としてシンタキシン 2D を同定した。シンタキシン 2D は IC_{50} 約 6 μM で、網膜血管内皮細胞の増殖を抑制した。網膜ペリサイト培養濃縮液による網膜血管内皮細胞増殖抑制メカニズムが PKC 介在型 p44/22MAPK シグナリング抑制であることを解明した。新規トロポミオシンの網膜血管内皮細胞増殖抑制機序は、網膜ペリサイト培養濃縮液で見られる機序と同様であり、網膜ペリサイトの網膜血管内皮細胞増殖抑制効果の一部を担っていることが示唆された。一方、シンタキシン 2D の内皮細胞増殖抑制機構は、主に細胞アポトーシスによることが明らかとなった。中性アミノ酸トランスポーターである LAT1 は新生血管内皮細胞に特に強く発現し、癌組織への必須アミノ酸供給に重要な役割を果たしているが、血液網膜関門の実体である網膜毛細血管内皮細胞には、LAT1 が特異的に発現していることを見いだした。糖尿病網膜症における網膜虚血状態の in vitro モデルとしてグルコース枯渇条件下で網膜血管内皮細胞を培養した結果、LAT1 mRNA 発現量の増加および基質である[^{3}H]L-leucine 取り込み速度の上昇、さらに LAT1 遺伝子 promoter 活性の上昇が示された。したがって、網膜血管内皮細胞には LAT1 を介した leucine など必須アミノ酸供給機構が機能し、さらに本機構はグルコース枯渇時には活性化することが示された。以上から、内皮細胞増殖抑制因子として新規トロポミオシンが同定され、網膜血管新生阻害剤の有力な標的分子として LAT1 を提示することができ、血管新生抑制治療法の開発につながっていくことが期待される。

分担研究者
立川　正憲　富山大学・大学院医学薬学研究部　助手（H17年度から）
笹岡　利安　富山大学・大学院医学薬学研究部　教授
登美　斉俊　富山大学・大学院医学薬学研究部　助手（H17年度まで）
寺崎　哲也　東北大学未来科学技術共同研究センター　教授（H16年度まで）

A．研究目的

高齢化社会を迎えた今日、糖尿病患者は約700万人いると言われており、その40-50%は網膜症を合併している。そのため、糖尿病網膜症は成人失明原因の第1位となっており、QOLの観点から糖尿病網膜症治療薬の社会的ニーズは極めて高いにもかかわらず、いままでに治療薬の開発はされていない。糖尿病網膜症における血管新生は、網膜血管の周囲にあるペリサイトの脱落から始まっており、網膜ペリサイトから分泌される因子が網膜血管内皮細胞の増殖を制御していると仮説を立てた。我々が樹立した網膜血管内皮細胞株(TR-iBRB)と網膜ペリサイト株(TR-rPCT)の共培養解析の結果、TR-rPCT細胞培養濃縮液をTR-iBRB細胞に添加すると増殖が著しく抑制されることを見いだした。そこで本研究では、網膜ペリサイトから分泌される網膜血管内皮細胞増殖抑制因子を同定し、網膜血管新生抑制機構を解明し、最終的には糖尿病網膜症治療薬の開発につなげることを目的とした。

B．研究方法

網膜ペリサイトから分泌される網膜血管内皮細胞増殖抑制因子を同定：TR-rPCT細胞培養濃縮液(rPCT-CM)から細胞増殖抑制因子を同定するため、rPCT-CMをゲルろ過法によってサイズ分画し、TR-iBRB細胞の増殖抑制活性を示した画分を二次元電気泳動法で分離した。さらに、MALDI-TOFMS、peptide mass fingerprinting (PMF)法を用いて、タンパク質の同定を行った。同定したタンパク質をコードする遺伝子をTR-rPCT細胞から単離後、大腸菌BL21に導入してリコンビナントタンパク質を作製し、TR-iBRB細胞増殖抑制効果の解析を行った。

網膜ペリサイトによる網膜血管内皮細胞増殖抑制機構：TR-rPCT細胞培養濃縮液(rPCT-CM)による網膜血管内皮細胞の遺伝子発現変動は、GeneChipを用いて網羅的に解析した。さらに、細胞周期関連タンパク質発現変動から網膜血管新生抑制機構を解析した。

網膜血管内皮細胞における中性アミノ酸トランスポーター(LAT)1の発現および発現変動解析：ラット大腿静脈から[^{3}H]L-leucineを投与した後、一定時間後に採血および臓器摘出を行い、[^{3}H]L-leucineの組織血漿間分配係数($K_{p,app}$)を算出した。さらに、integration plot法を用いて見かけの[^{3}H]L-leucine網膜取り込みクリアランスを算出した。TR-iBRB細胞におけるL-leucine輸送機構は、37°Cにおける[^{3}H]L-leucine取り込みから解析した。網膜血管内皮細胞は、ラット網膜ホモジネート

を酵素処理後、磁気標識抗 CD31 抗体と混合して内皮細胞を磁気標識し、磁石を用いて単離した。LAT1 の発現は免疫染色法、Western blot 法、RT-PCR 法、およびリアルタイム定量 PCR 法を用いて解析した。ラットゲノム DNA ライブラリーから PCR 法を用いて LAT1 遺伝子プロモーター配列(-1958/+70)を増幅し、ルシフェラーゼ遺伝子を有する pGL3-Basic プラスミドに挿入した(LAT1 promoter/pGL3 プラスミド)。構築したプラスミドを TR-iBRB 細胞に導入し、ルミノメーターを用いたルシフェラーゼアッセイにより LAT1 プロモーター活性を測定した。

(倫理面への配慮) いずれの研究も、動物実験のみでヒトの材料を使った研究は行われていない。ヒト臍帯静脈内皮細胞およびヒト網膜血管内皮細胞は研究用に販売されているもの (Toyobo, Osaka) を購入して用いた。DNA 組替え実験については、第二種使用拡散防止措置 (組換え DNA 実験指針) に対応した富山大学・DNA 安全委員会の承認を得ている。動物実験に際しては Association for Research of Vision and Ophthalmology (ARVO)決議を順守し、富山大学・動物実験委員会から承認を受けて行った。

C. 研究結果および考察

網膜ペリサイトによる網膜血管内皮細胞増殖抑制機構：ペリサイトの液性因子が内皮細胞に対して及ぼす影響を解析するために、rPCT-CM を TR-iBRB 細胞に添加した結果、TR-iBRB 細胞の増殖は rPCT-CM の濃度依存的に抑制された。ヒト臍帯静脈内皮細胞およびヒト網膜血管内皮細胞の増殖についても 5 倍濃縮 rPCT-CM 添加で抑制された一方、T 抗原遺伝子導入不死化細胞株 COS7 の増殖には影響を与えなかった。5 倍濃縮 rPCT-CM 添加時の TR-iBRB 細胞における細胞周期制御タンパク質への影響を Western blot 法によって解析した。その結果、cyclin D1、cyclin-dependent kinase 4 (cdk4)、cdk6 の発現は 5 倍濃縮 rPCT-CM を添加することで減少した。DNA-polymerase-δ associated protein である proliferating cell number antigen (PCNA)の発現も 5 倍濃縮 rPCT-CM を添加した TR-iBRB 細胞において減少する傾向を示した。さらに、TR-iBRB 細胞における 5-bromo-2'-deoxyuridine (BrdU)の取り込み量を測定したところ、rPCT1-CM の濃度依存的に BrdU 取り込みが減少し、DNA 合成が抑制されていることが示された。

細胞増殖は細胞外からの増殖促進因子の刺激によって誘導される。そこで rPCT1-CM が FBS による増殖促進シグナルを抑制するかどうかを Western blot 法によって検討した。TR-iBRB 細胞に 10% FBS DMEM を添加したところ、protein kinase C (PKC) α/βII および p44/22 mitogen-activated protein kinase (MAPK)が活性化された。しかし、10% FBS を含む 5 倍濃縮 rPCT-CM を添加すると、PKC α/βII および p44/22 MAPK のリン酸化体が短時間で減少する傾向を示した。一方、protein kinase B (Akt)は 10% FBS DMEM を添加してもリン酸化体はほとんど検出されず、10% FBS を含む 5 倍濃縮 rPCT-CM によっても活性化されなかった。

網膜ペリサイトから分泌される網膜血管内皮細胞増殖抑制因子を同定：TR-rPCT 細胞の培養濃縮液タンパクは 60 のフラクショ

ンに分離した。60のフラクションの中でNo. 25およびNo. 31-35のフラクション付近で細胞増殖の指標に用いたBrdUの強い取り込み抑制が示された。このフラクションタンパク質を2次元電気泳動にて分離し、MALDI-TOFMS、PMF解析からトロポミオシン(TM)およびシンタキシン2Dであることが示唆された。TMタンパク質は、今までに報告されているTM3、TM6およびTMαと相同性が高いものの、これらとは一致しない配列であった。ラットTM3、TM6およびシンタキシン2Dを特異的に認識するプライマーを用いてRT-PCR法でオープンリーディングフレーム（ORF）のクローニングを行った。その結果、ラット網膜およびTR-rPCT細胞に新規に単離したTMタンパク質およびシンタキシン2DをコードするmRNAが発現していることが示された。TMにおいては、増幅されたPCR産物の遺伝子配列から予想されるアミノ酸配列からもTM3、TM6およびTMαとは異なるタンパク質であることが示唆された。シンタキシン2アイソフォームを認識する抗体を用いた解析から、シンタキシン2DはTR-rPCT細胞に発現し、培養液中にも存在していることが示唆された。

新規に単離されたTMタンパク質およびシンタキシン2Dのリコンビナント体を作製するために、目的遺伝子のORFを発現誘導ベクターに導入し、大腸菌にて大量に培養した。タンパク質は大腸菌から収集、精製した。精製したタンパク質はMALDI-TOFMSによってタンパク質量を、プロテインシークエンサーを用いてN末端アミノ酸配列解析を行い単離したタンパク質と同一であることを確認した。

得られた新規に単離したTMタンパク質の内皮細胞増殖抑制効果は、TR-iBRB細胞を用いて解析した。TR-rPCT細胞の5倍培養濃縮液をコントロールにして測定したところ、新規に単離したTMタンパク質およびシンタキシン2Dは濃度依存的にTR-iBRB細胞の増殖を抑制し、IC_{50}値はそれぞれ約2 μMおよび6 μMであった。一方、ウシ血清アルブミンを添加した場合、細胞増殖抑制効果は示されなかったことから、新規に単離したTMタンパク質およびシンタキシン2Dの内皮細胞増殖抑制効果は特異的であることが示唆された。

TR-iBRB細胞に、新規に単離したTMタンパクを10 μMで添加するとG1期からS期への移行を促進するcdk4、cdk6およびこれら2つのcdkと複合体を形成して細胞周期促進するcyclin D1の発現を減少させた。さらに、PCNAの発現も減少させた。一方、10 μMシンタキシン2Dの添加においては、cdk4の発現減少が示されたものの、他の細胞周期タンパク質には影響を与えなかった。シンタキシン2DはTR-iBRB細胞にアポトーシスを誘導することが示された。

TR-iBRB細胞をrPCT-CMで処理すると、plasminogen activator, urokinase、inhibitor of DNA binding 1、growth arrest and DNA-damage-inducible 45β、activating transcription factor 3などを含む68遺伝子が4倍以上の発現変動を示し、rPCT-CMがplasminogen activator inhibitorやthrombospondinを介した血管新生の制御に関わることが示唆された。一方、遺伝子解析では、TGF-βによって有意な発現変動を示した遺伝子はその一部に留まった。抗TGF-β中和抗体を用いたrPCT-CMによるTR-iBRB細胞増殖抑制効果

解析から、TGF-βの関与は一部であることが明らかとなっており、網膜ペリサイト細胞分泌因子には TGF-βとは異なる細胞増殖抑制因子が存在し、細胞周期や基底膜分解に関わる複数の経路を制御することで細胞増殖を抑制していることが示唆された。

LAT1 の発現および発現変動解析：ラット網膜への L-leucine 移行性を解析するため、integration plot 法を用いた in vivo 解析を行った。見かけの[^{3}H]L-leucine 網膜取り込みクリアランスは 203 μL/(min･g retina)であることが示された。

TR-iBRB 細胞における[^{3}H]L-leucine 取り込みは 10 分までは直線性を示し、その取り込みは Na^+および Cl^-非依存性を示した。TR-iBRB 細胞における L-leucine 取り込みは濃度依存性を示し、得られた Michaelis-Menten 定数は 14.1 μM であった。さらに、[^{3}H]L-leucine の取り込みは LAT1、LAT2 に共通の基質である L-leucine、L-phenylalanine、L-methionine、L-valine、L-isoleucine、L-tyrosine、L-tryptophan および 2-aminobicyclo-(2,2,1)-heptane-2-carboxylic acid (BCH)に加え、LAT1 のみの基質である D-leucine、D-phenylalanine および D-methionine によって 50%以上阻害された。一方、LAT2 のみの基質である L-alanine および L-glutamine によっては 30%程度の阻害にとどまった。

磁気標識抗 CD31 抗体を用いて単離した網膜血管内皮細胞および TR-iBRB 細胞において LAT1 および LAT2 mRNA の発現が共に示されたが、LAT1 mRNA の発現量は LAT2 と比較して各々15 倍および 100 倍高いことが示された。TR-iBRB 細胞および初代培養ヒト網膜血管内皮細胞には LAT1 タンパク質が発現していることが示された。さらに、凍結網膜切片に対する免疫染色解析から、in vivo ラット網膜毛細血管内皮細胞に LAT1 が発現していることが示された。

酸素濃度 1%の低酸素条件およびグルコース非含有培地を用いた glucose 枯渇条件のそれぞれで培養した TR-iBRB 細胞を虚血状態の in vitro モデルとした。低酸素条件下で 24 時間培養した TR-iBRB 細胞において、LAT1 mRNA の発現量は変動せず、[^{3}H]L-leucine の取り込みについても 1.6 倍の増加であった。一方、グルコース枯渇条件下における LAT1 mRNA の発現、および[^{3}H]L-leucine の取り込みは処理時間依存的に増加し、処理時間 24 時間において LAT1 mRNA は 4.0 倍、および[^{3}H]L-leucine の取り込みは 2.6 倍に増加した。グルコース枯渇条件下における mRNA 発現誘導および取り込み活性化は転写阻害剤 actinomycin D によって抑制され、取り込み活性化については翻訳阻害剤 cycloheximide によっても抑制された。

LAT1 promoter/pGL3 プラスミドを導入した TR-iBRB 細胞においてルシフェラーゼアッセイを用いた転写活性解析を行った結果、control プラスミド導入細胞に比べて数十倍高い転写活性が示された。さらに、グルコース枯渇条件下では通常培養条件と比較して 2 倍高いことが示された。以上から、虚血時に LAT1 が誘導され、必須アミノ酸が供給されて血管新生につながることが示唆された。

D. 結論

本研究によって、網膜ペリサイトから分泌される網膜血管内皮細胞増殖因子の１つとして新規トロポミオシンの関与を明らかにした。新規トロポミオシンの内皮細胞増殖抑制機構として、cyclin D1、cdk4、cdk6の発現を減少させることで細胞周期のG1/S期の移行を制御していることが明らかとなった。

網膜ペリサイト細胞分泌因子にはTGF-βとは異なる細胞増殖抑制因子が存在し、細胞周期や基底膜分解に関わる複数の経路を制御することで総合的に細胞増殖を抑制していることが示唆された。

本研究によって、網膜血管内皮細胞にはLAT1が発現し、leucineなど必須アミノ酸の輸送を担っていることが示唆された。さらに、グルコース枯渇時にはLAT1遺伝子の転写が活性化し、その発現が誘導されることが示された。したがって、LAT1は虚血とそれに伴う血管新生時における旺盛なアミノ酸需要に応える役割を果たしている可能性が高い。以上から、LAT1を標的分子とした阻害剤を開発し、網膜血管内皮細胞への必須アミノ酸供給を遮断することで血管新生を抑制するという、網膜血管新生治療に向けた新戦略を提示することができた。

E. 健康危険情報

特になし

F. 研究発表

１．論文発表

Ohtsuki S, Tomi M, Hata T, Nagai Y, Hori S, Mori S, Hosoya K, Terasaki T, Dominant expression of androgen receptor and its functional regulation of organic anion transporter 3 in rat brain capillary endothelial cells; comparison of gene expression between the blood-brain and -retinal barriers. *J. Cell. Physiol.*, 204, 896-900 (2005).

Fukui K, Wada T, Kagawa S, Nagira K, Ikubo M, Ishihara H, Kobayashi M, Sasaoka T, Impact of the liver-specific expression of SHIP2 (SH2-containing inositol 5'-phosphatase 2) on insulin signaling and glucose metabolism in mice. *Diabetes*, 54, 1958-1967 (2005)

Nakashima T, Tomi M, Tachikawa M, Watanabe M, Terasaki T, Hosoya K, Evidence for creatine biosynthesis in Müller glia. *Glia*, 52, 47-52 (2005).

Zhou J, Deo BK, Hosoya K, Terasaki T, Obrosova IG, Brosius III FC, Kumagai AK, Increased JNK phosphorylation and oxidative stress in response to increased glucose flux through increased GLUT1 expression in rat retinal endothelial cells. *Invest. Ophthalmol. Vis. Sci.*, 46, 3403-3410 (2005).

Hori S, Ohtsuki S, Hosoya K, Nakashima E, Terasaki T. A pericyte-derived angiopoietin-1 multimeric complex induces occludin gene expression in brain capillary endothelial cells through Tie-2 activation in vitro. *J. Neurochem.*, 89, 503-513 (2004).

Hori S, Ohtsuki S, Tachikawa M, Kimura N, Kondo T, Watanabe M, Emi Nakashima, Terasaki T. Functional expression of rat ABCG2 on the luminal side of brain capillaries and its enhancement by astrocyte-derived soluble factor(s). *J. Neurochem.*, 90, 526-536 (2004).

Kondo T, Hosoya K, Hori S, Tomi M, Ohtsuki S, Terasaki T. PKC/MAPK signaling suppression by retinal pericyte conditioned medium prevents retinal endothelial cell proliferation. *J. Cell. Physiol.*, 203, 378-386 (2005).

Ohtsuki S, Tomi M, Hata T, Nagai Y, Hori S, Mori S, Hosoya K, Terasaki T, Dominant expression of androgen receptor and its functional regulation of organic anion transporter 3 in rat brain capillary endothelial cells; comparison of gene expression between the blood-brain and -retinal barriers. *J. Cell. Physiol.*, 204, 896-900 (2005).

Fukui K, Wada T, Kagawa S, Nagira K, Ikubo M, Ishihara H, Kobayashi M, Sasaoka T, Impact of the liver-specific expression of SHIP2 (SH2-containing inositol 5'-phosphatase 2) on insulin signaling and glucose metabolism in mice. *Diabetes*, 54, 1958-1967 (2005)

Nakashima T, Tomi M, Tachikawa M, Watanabe M, Terasaki T, Hosoya K, Evidence for creatine biosynthesis in Müller glia. *Glia*, 52, 47-52 (2005).

Zhou J, Deo BK, Hosoya K, Terasaki T, Obrosova IG, Brosius III FC, Kumagai AK, Increased JNK phosphorylation and oxidative stress in response to increased glucose flux through increased GLUT1 expression in rat retinal endothelial cells. *Invest. Ophthalmol. Vis. Sci.*, 46, 3403-3410 (2005).

Tomi M, Mori M, Tachikawa M, Katayama K, Terasaki T, Hosoya K. L-Type amino acid transporter 1 (LAT1)-mediated L-leucine transport at the inner blood-retinal barrier. *Invest. Ophthalmol. Vis. Sci.*, 46, 2522-2530 (2005).

Nagase K, Tomi M, Tachikawa M, Hosoya K. Functional and molecular characterization of adenosine transport at the rat inner blood-retinal barrier. *Biochim. Biophys. Acta*, 1758, 13-19 (2006).

Katayama K, Ohshima Y, Tomi M, Hosoya K. Application of microdialysis to evaluate the efflux transport of estradiol 17-▪ glucuronide across the rat blood-retinal barrier. *J. Neurosci. Methods*, 156, 249-256 (2006).

Minamizono A, Tomi M, Hosoya K. Inhibition of dehydroascorbic acid transport across the rat blood-retinal

and -brain barriers in experimental diabetes. *Biol. Pharm. Bull.*, 29, 2148-2150 (2006).

Nagira K, Sasaoka T, Wada T, Fukui K, Ikubo M, Hori S, Tsuneki H, Saito S, Kobayashi M. Altered subcellular distribution of estrogen receptor alpha is implicated in estradiol-induced dual regulation of insulin signaling in 3T3-L1 adipocytes. *Endocrinology*, 147, 1020-1028 (2006).

Ikesugi K, Mulhern ML, Madson CJ, Hosoya K, Terasaki T, Kador PK, Shinohara T. Induction of endoplasmic reticulum stress in retinal pericytes by glucose deprivation. *Curr Eye Res.*, 31, 947-953 (2006).

H．知的財産権の出願・登録情報

１．特許取得

細谷健一，寺崎哲也，大槻純男，登美斉俊：網膜周皮細胞由来の細胞増殖抑制因子，特開 2006-238844.

２．実用新案登録　なし

３．その他　なし

研究成果の刊行に関する一覧表

発表者氏名	論文タイトル名	発表誌名	巻号	ページ	出版年
Hosoya K, Minamizono A, Katayama K, Terasaki T, Tomi M.,	Vitamin C transport in oxidized form across the rat blood-retinal barrier.	*Invest. Ophthalmol. Vis. Sci.*	45	1232-1239	2004
Sasaoka T, Wada T, Fukui K, Murakami S, Ishihara H, Suzuki R, Tobe K, Kadowaki T, Kobayashi M.	SH2-containing inositol phosphatase 2 predominantly regulates Akt2, and not Akt1, phosphorylation at the plasma membrane in response to insulin in 3T3-L1 adipocytes.	*J. Biol. Chem.*	279	14835-14843	2004
Nakashima T, Tomi M, Katayama K, Tachikawa M, Watanabe M, Terasaki T, Hosoya K.	Blood-to-retina transport of creatine via creatine transporter (CRT) at the rat inner blood-retinal barrier.	*J. Neurochem.*	89	1454-1461	2004
Tomi M, Abukawa H, Nagai Y, Hata T, Takanaga H, Ohtsuki S, Terasaki T, Hosoya K.	Retinal selectivity of gene expression in rat retinal versus brain capillary endothelial cell lines by differential display analysis.	*Mol. Vis.*	10	537-543	2004
Fernandes R, Carvalho AL, Kumagai A, Seica R, Hosoya K, Terasaki T, Murta J, Pereira P, Faro C.	Downregulation of retinal GLUT1 in diabetes by ubiquitinylation.	*Mol. Vis.*	10	618-628	2004
Hori S, Ohtsuki S, Hosoya K, Nakashima E, Terasaki T.	A pericyte-derived angiopoietin-1 multimeric complex induces occludin gene expression in brain capillary endothelial cells through Tie-2 activation in vitro.	*J. Neurochem.*	89	503-513	2004
Hori S, Ohtsuki S, Tachikawa M, Kimura N, Kondo T, Watanabe M, Emi Nakashima, Terasaki T.	Functional expression of rat ABCG2 on the luminal side of brain capillaries and its enhancement by astrocyte-derived soluble factor(s).	*J. Neurochem.*	90	526-536	2004
Tomi M, Hosoya K.	Application of magnetically isolated rat retinal vascular endothelial cells for the determination of transporter gene expression levels at the inner blood-retinal barrier.	*J. Neurochem.*	91	1244-1248	2004

Hosoya K, Tomi M.	Advances in the cell biology of transport via the inner blood-retinal barrier: establishment of cell lines and transport functions.	*Biol. Pharm. Bull.*	28	1-8	2005
Kondo T, Hosoya K, Hori S, Tomi M, Ohtsuki S, Terasaki T.	PKC/MAPK signaling suppression by retinal pericyte conditioned medium prevents retinal endothelial cell proliferation.	*J. Cell. Physiol*	203	378-386	2005
Ohtsuki S, Tomi M, Hata T, Nagai Y, Hori S, Mori S, Hosoya K, Terasaki T.	Dominant expression of androgen receptor and its functional regulation of organic anion transporter 3 in rat brain capillary endothelial cells; comparison of gene expression between the blood-brain and -retinal barriers.	*J. Cell. Physiol.*	204	896-900	2005
Fukui K, Wada T, Kagawa S, Nagira K, Ikubo M, Ishihara H, Kobayashi M, Sasaoka T.	Impact of the liver-specific expression of SHIP2 (SH2-containing inositol 5'-phosphatase 2) on insulin signaling and glucose metabolism in mice.	*Diabetes*	54	1958-1967	2005
Nakashima T, Tomi M, Tachikawa M, Watanabe M, Terasaki T, Hosoya K.	Evidence for creatine biosynthesis in Müller glia.	*Glia*	52	47-52	2005
Zhou J, Deo BK, Hosoya K, Terasaki T, Obrosova IG, Brosius III FC, Kumagai AK.	Increased JNK phosphorylation and oxidative stress in response to increased glucose flux through increased GLUT1 expression in rat retinal endothelial cells.	*Invest. Ophthalmol. Vis. Sci.*	46	3403-3410	2005
Tomi M, Mori M, Tachikawa M, Katayama K, Terasaki T, Hosoya K.	L-type amino acid transporter 1-mediated L-leucine transport at the inner blood-retinal barrier	*Invest. Ophthalmol. Vis. Sci.*	10	2522-2530	2005
Nagase K, Tomi M, Tachikawa M, Hosoya K.	Functional and molecular characterization of adenosine transport at the rat inner blood-retinal barrier.	*Biochim. Biophys. Acta*	1758	13-19	2006
Katayama K, Ohshima Y, Tomi M, Hosoya K.	Application of microdialysis to evaluate the efflux transport of estradiol 17-β glucuronide across the rat blood-retinal barrier.	*J. Neurosci. Methods*	156	249-256	2006

Minamizono A, Tomi M, Hosoya K.	Inhibition of dehydroascorbic acid transport across the rat blood-retinal and -brain barriers in experimental diabetes.	*Biol. Pharm. Bull.*	29	2148-2150	2006
Nagira K, Sasaoka T, Wada T, Fukui K, Ikubo M, Hori S, Tsuneki H, Saito S, Kobayashi M.	Altered subcellular distribution of estrogen receptor alpha is implicated in estradiol-induced dual regulation of insulin signaling in 3T3-L1 adipocytes.	*Endocrinology*	147	1020-1028	2006
Ikesugi K, Mulhern ML, Madson CJ, Hosoya K, Terasaki T, Kador PK, Shinohara T.	Induction of endoplasmic reticulum stress in retinal pericytes by glucose deprivation.	*Curr. Eye Res.*	31	947-953	2006

Vitamin C Transport in Oxidized Form across the Rat Blood–Retinal Barrier

Ken-ichi Hosoya,[1,2] *Akito Minamizono,*[1] *Kazunori Katayama,*[1] *Tetsuya Terasaki,*[2-4] *and Masatoshi Tomi*[1,2]

Purpose. To elucidate the mechanisms of vitamin C transport across the blood-retinal barrier (BRB) in vivo and in vitro.

Methods. [^{14}C]Dehydroascorbic acid (DHA) and [^{14}C]ascorbic acid (AA) transport in the retina across the BRB were examined using in vivo integration plot analysis in rats, and the transport mechanism was characterized using a conditionally immortalized rat retinal capillary endothelial cell line (TR-iBRB2) as an in vitro model of the inner BRB.

Results. The apparent influx permeability clearance (K_{in}) per gram of retina of [^{14}C]DHA and [^{14}C]AA was found to be 2.44×10^3 μL/(min · g retina) and 65.4 μL/(min · g retina), respectively. In the retina and brain, the K_{in} of [^{14}C]DHA was approximately 38 times greater than that of [^{14}C]AA, whereas there was no major difference in the heart. The K_{in} of [^{14}C]DHA in the retina was eight times greater than that in the brain. HPLC analysis revealed that most of the vitamin C accumulated in AA form in the retina. These results suggest that vitamin C is mainly transported in DHA form across the BRB and accumulates in AA form in the rat retina. In an in vitro uptake study in TR-iBRB2 cells, the initial uptake rate of [^{14}C]DHA was 37 times greater than that of [^{14}C]AA, which is in agreement with the results of the in vivo study. [^{14}C]DHA uptake by TR-iBRB2 cells took place in an Na^+-independent and concentration-dependent manner with a K_m of 93.4 μM. This process was inhibited by substrates and inhibitors of glucose transporters. [^{14}C]DHA uptake was inhibited by D-glucose in a concentration-dependent manner with a 50% inhibition concentration of 5.56 mM. Quantitative real-time PCR and immunostaining analyses revealed that expression of GLUT1 and -3 was greater than that of the Na^+-dependent L-ascorbic acid transporter (SVCT)-2 in TR-iBRB2 cells.

Conclusions. Vitamin C is mainly transported across the BRB as DHA mediated through facilitative glucose transporters and accumulates as AA in the rat retina. (*Invest Ophthalmol Vis Sci.* 2004;45:1232-1239) DOI:10.1167/iovs.03-0505

Vitamin C, which is an essential substance in humans, acts as a cofactor in the enzymatic biosynthesis of collagen, catecholamine, and peptide neurohormones and as an antioxidant and/or free radical scavenger to detoxify free radicals in body tissues.[1] The retina is the only tissue in which light is focused on a group of cells. It is necessary to protect the retina against oxidative stress because light causes free radical oxidation.[2] Vitamin C is present in the retina at a high concentration compared with its presence in other organs in humans.[1,3] The concentration of L-ascorbic acid (AA) is approximately 1.6 mM in the rat and guinea pig retina, although the plasma concentration in most mammals is 50 to 100 μM,[3,4] suggesting that AA is transported from the circulating blood to the retina across the blood-retinal barrier (BRB) through a specific transport process. Possible sources of oxidative stress in diabetes and retinal diseases include increased generation of reactive oxygen species by autooxidation of D-glucose and a reduced tissue concentration of antioxidants.[5,6] It is important to elucidate the transport mechanisms for vitamin C as far as the supply of antioxidants in the neural retina is concerned.

The BRB, which is composed of retinal capillary endothelial cells (inner BRB) and retinal pigmented epithelial cells (RPE, outer BRB), plays a key role in restricting the nonspecific transport of hydrophilic compounds and facilitating the influx and efflux transport of essential molecules and xenobiotics, respectively, from the circulating blood to the retina and vice versa.[7,8] Na^+-dependent L-ascorbic acid transporter (SVCT)-1 and -2 have been cloned and mediate concentrated, high-affinity AA transport that is driven by the Na^+ electrochemical gradient.[9] Although SVCT2 mRNA is present in the retina,[9] its localization and transport functions are not fully understood. An Na^+-dependent L-ascorbic acid transport process and SVCT2 are present in RPE[10] and lens epithelial cells,[11] respectively. However, the Na^+-dependent L-ascorbic acid transport process in RPE is inhibited by D-glucose, suggesting that it may not be SVCT1 or -2.[10] The facilitative glucose transporters, GLUT1 and -3 mediate equilibrative and relatively low-affinity dehydroascorbic acid (DHA) transport.[12,13] DHA is an oxidized form of AA, and its plasma concentration is reported to be approximately 10 μM in the rat[14] and human.[15] Agus et al.[16] have reported that DHA crosses the blood-brain barrier (BBB) through GLUT1 at the luminal and abluminal side of BBB and accumulates as reduced AA in the brain. Although GLUT1 is expressed at both the inner BRB and RPE and plays an essential role in supplying D-glucose as an energy source in the neural retina,[17,18] our knowledge of vitamin C transport mechanism across the BRB is incomplete.

The purpose of this study was to elucidate the mechanisms of vitamin C transport across the BRB. To be able to understand the physiological and pathophysiological roles of BRB transport, we wanted to discover whether SVCT2 or glucose transporters make the greatest contribution to the supply of vitamin C to the retina.

From the [1]Faculty of Pharmaceutical Sciences, Toyama Medical and Pharmaceutical University, Toyama, Japan; [2]Core Research for Evolutional Science and Technology (CREST), Japan Science and Technology Corp., Japan; the [3]Department of Molecular Biopharmacy and Genetics, Graduate School of Pharmaceutical Sciences, and the [4]New Industry Creation Hatchery Center, Tohoku University, Sendai, Japan.

Supported in part by a Grant-in-Aid for Scientific Research from Japan Society for the Promotion of Science, the Nakatomi Foundation, the Suzuken Memorial Foundation, and the Mochida Memorial Foundation for Medical and Pharmaceutical Research.

Submitted for publication May 22, 2003; revised August 9 and December 25, 2003; accepted January 5, 2004.

Disclosure: **K.-i. Hosoya**, None; **A. Minamizono**, None; **K. Katayama**, None; **T. Terasaki**, None; **M. Tomi**, None

The publication costs of this article were defrayed in part by page charge payment. This article must therefore be marked "*advertisement*" in accordance with 18 U.S.C. §1734 solely to indicate this fact.

Corresponding author: Ken-ichi Hosoya, Faculty of Pharmaceutical Sciences, Toyama Medical and Pharmaceutical University, 2630, Sugitani, Toyama 930-0194, Japan; hosoyak@ms.toyama-mpu.ac.jp.

Investigative Ophthalmology & Visual Science, April 2004, Vol. 45, No. 4

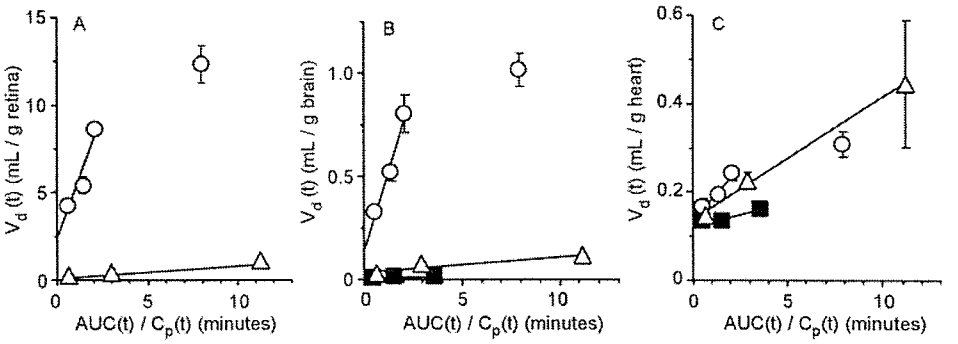

FIGURE 1. Integration plot of the initial uptake of [^{14}C]DHA, [^{14}C]AA, and [^{3}H]D-mannitol by the retina (**A**), brain (**B**), and heart (**C**) after intravenous administration. [^{14}C]DHA (○, 5 μCi/rat), [^{14}C]AA (△, 10 μCi/rat), or [^{3}H]D-mannitol (■, 10 μCi/rat) was injected into the femoral vein. The counts of [^{3}H]D-mannitol uptake by the retina were close to background. Each point represents the mean ± SEM (n = 3–5).

MATERIALS AND METHODS

Animals

Male Wistar rats, weighing 250 to 300 g, were purchased from SLC (Shizuoka, Japan). The investigations using rats described in this report conformed to the provisions of the Animal Care Committee, Toyama Medical and Pharmaceutical University (2001-190) and the ARVO Statement for the Use of Animals in Ophthalmic and Vision Research.

Reagents

L-[1-^{14}C]Ascorbic acid ([^{14}C]AA, 13 mCi/mmol) and D-[1-^{3}H(*N*)]mannitol ([^{3}H]D-mannitol, 17 Ci/mmol) were purchased from PerkinElmer Life Sciences (Boston, MA). L-[^{14}C]Dehydroascorbic acid ([^{14}C]DHA, purity more than 90%; see Fig. 2B) was generated in all experiments by incubating [^{14}C]AA (1 μM in saline) with ascorbate oxidase (1 unit/1 mmol AA in saline; Sigma-Aldrich, St. Louis, MO) at 37°C for 90 seconds, according to a reported method.[16] All other chemicals were of reagent grade and available commercially.

Blood-to-Retina Transport Studies

A Wistar rat was anesthetized with an intramuscular injection of ketamine-xylazine (1.22 mg/kg xylazine and 125 mg/kg ketamine). The femoral artery was cannulated with polyethylene tubing (SP-31, inner diameter 0.5 mm, outer diameter 0.8 mm; Natsume, Tokyo, Japan) containing 100 IU heparin/mL in extracellular fluid buffer (122 mM NaCl, 25 mM $NaHCO_3$, 3 mM KCl, 1.4 mM $CaCl_2$, 1.2 mM $MgSO_4$, 0.4 mM K_2HPO_4, 10 mM D-glucose, and 10 mM HEPES [pH 7.4]) to collect blood samples. Then, [^{14}C]DHA (5 μCi/rat), [^{14}C]AA (10 μCi/rat), or [^{3}H]D-mannitol (10 μCi/rat) was injected into the femoral vein. After collection of blood samples, all rats were decapitated, and the retinas, cerebrum, and heart were removed. All samples were dissolved in 2 N NaOH at 50°C for 3 hours. After the samples were dissolved, 50 μL H_2O_2 was added to the blood and heart samples to decolorize them. All samples were neutralized and mixed with liquid scintillation cocktail (ACS II; Amersham, Buckinghamshire, UK) and then the radioactivity was measured in a liquid scintillation counter (LS6500; Beckman-Coulter, Fullerton, CA).

Determination of Influx Permeability Clearance

The apparent influx permeability clearance (K_{in}) of [^{14}C]DHA, [^{14}C]AA, or [^{3}H]D-mannitol in tissues was determined by integration plot analysis,[19,20] by modification of a reported method.[20] Briefly, the tissue uptake of each compound can be expressed as

$$dX(t)/dt = K_{in} \times C_p(t) - K_{eff} \times X(t) \quad (1)$$

where $X(t)$ (dpm/g tissue) and $C_p(t)$ (dpm/mL) are the tissue concentration and plasma concentration at time t, respectively, and K_{in} and K_{eff} represent the influx and efflux permeability clearance in tissue, respectively. Integrating equation 1 and solving the apparent tissue concentration in the early-phase gives

$$X_{app}(t) = K_{in} \times AUC(t) + V_i \times C_p(t) \quad (2)$$

where $X_{app}(t)$ (dpm/g tissue) is the apparent tissue concentration in the sample, AUC(t) (dpm · min/mL) is the area under the plasma concentration time curve of each compound from time 0 to t and V_i (mL/g tissue) is the volume of interstitial space in the tissue. Division of both sides of equation 2 by $C_p(t)$ gives

$$X_{app}(t)/C_p(t) = K_{in} \times AUC(t)/C_p(t) + V_i \quad (3)$$

The apparent tissue-to-plasma concentration ratio [$V_d(t)$] (mL/g tissue) is defined as $X_{app}(t)/C_p(t)$

$$V_d(t) = K_{in} \times AUC(t)/C_p(t) + V_i \quad (4)$$

when $AUC(t)/C_p(t)$ (minute) is plotted versus $V_d(t)$, as shown in Figure 1, the early-phase slope represents the K_{in} in the tissue (μL/(min · g tissue)). The apparent influx permeability clearances of [^{14}C]DHA, [^{14}C]AA, or [^{3}H]D-mannitol in retina ($K_{in,\ retina}$), brain ($K_{in,\ brain}$), and heart ($K_{in,\ heart}$) were determined.

High-Performance Liquid Chromatography Analysis

The purity of [^{14}C]DHA prepared in each experiment, and the metabolism of [^{14}C]DHA in plasma and retina were determined by high-performance liquid chromatography (HPLC). Thirty seconds or 5 minutes after intravenous injection, plasma and retinas were collected and frozen with dry ice. The frozen sample of retina was homogenized in 70% MeOH, and plasma was mixed with 70% MeOH. After centrifugation at 12,550*g* for 5 minutes, an aliquot of the samples was subjected to HPLC, using a system equipped with an anion exchange column (TSK-Gel NH_2-60; Tosoh, Tokyo, Japan). The mobile phase consisted of 35% 0.05 M KH_2PO_4-65% CH_3CN at a flow rate of 1.0 mL/min. The eluent was collected in vials, and the radioactivity in each fraction was determined by liquid scintillation counting.

[^{14}C]DHA and [^{14}C]AA Uptake by TR-iBRB2 Cells

The conditionally immortalized rat retinal capillary endothelial cell line (TR-iBRB2), which had been established and characterized,[21–23] was used as an in vitro inner BRB model to characterize DHA and AA transport. TR-iBRB2 cells express GLUT1 protein and have functional 3-O-methyl-D-glucose (3-OMG) transport, with a K_m of 5.56 mM.[21] TR-iBRB2 cells (passages 27–38) were cultured at 33°C in Dulbecco's modified Eagle's medium (Nissui Pharmaceutical Co., Tokyo, Japan) in 5% CO_2-air, as described previously.[21] For the uptake study, cells (5×10^4 cells/cm^2) were cultured at 33°C for 2 days on a rat tail collagen-type I-coated 24-well plate (BD Biosciences, San Jose, CA) and washed with 1 mL uptake buffer (134 mM NaCl, 5.2 mM KCl, 0.8 mM $MgSO_4$, 1.8 mM $CaCl_2$, and 20 mM HEPES [pH 7.5]) at 37°C. Uptake was initiated by applying 200 μL uptake buffer containing 0.2 μCi [^{14}C]DHA (69.2 μM) or [^{14}C]AA (76.9 μM) at 37°C in the presence or

absence of inhibitors. For the concentration-dependent study, a concentration range of DHA from 1.7 to 180 μM was prepared using [^{14}C]DHA from 4.9 nCi to 4.4 μCi. Na^+-free uptake buffers were prepared in two different ways. The choline- and Li^+-buffers were prepared by equimolar replacement of NaCl with choline chloride and LiCl, respectively. After a predetermined time period, uptake was terminated by removing the solution, and cells were immersed in ice-cold uptake buffer and solubilized. [^{14}C]DHA in the uptake buffer was stable over the uptake study period of 3 minutes. Radioactivity was measured by liquid scintillation counting, and the protein content was determined with a kit (DC; Bio-Rad, Hercules, CA) with bovine serum albumin (BSA) as a standard.

RT-PCR Analysis

Total cellular RNA was prepared from phosphate-buffered saline (PBS)-washed cells using a kit (RNeasy Mini Kit; Qiagen, Hilden, Germany). Single-strand cDNA was made from 1 μg total RNA by reverse transcription (RT), using oligo dT primer. The polymerase chain reaction (PCR) was performed with a gene amplification system (GeneAmp PCR system 9700; Applied Biosystems, Foster City, CA) with GLUT1-, GLUT3-, SVCT1-, SVCT2-, and β-actin–specific primers through 25 cycles of 94°C for 30 seconds, 60°C for 1 minute, and 72°C for 1 minute. The sequences of the specific primers were as follows: sense, 5′-GAT GAT GAA CCT GTT GGC CT-3′; antisense, 5′-AGC GGA CAG CTC CAA GAT G-3′ for rat GLUT1 (Slc2a1, GenBank accession number NM_138827; http://www.ncbi.nlm.nih.gov/Genbank; provided in the public domain by the National Center for Biotechnology Information, Bethesda, MD); sense, 5′-GAC GAG AGT ATC AGG ATG TCA CAG-3′; antisense, 5′-AGG CCA CGT AGA CCA AGA TAG CC-3′ for rat GLUT3 (Slc2a3, GenBank accession number NM_017102); sense, 5′-CCT GTT TAC CGA TGG GGC AAG G-3′ antisense, 5′-ACT CGA TGA TGC CCG CCA GTG T-3′ for rat SVCT1 (Slc23a2, GenBank accession number NM_017316); sense, 5′-ACA CCA CAG AGA TCA CAG TTG CC-3′; antisense, 5′-TGT AAC TTG TAG GCC GTC CAT CC-3′ for rat SVCT2 (Slc23a1, GenBank accession number NM_017315); sense, 5′-TCA TGA AGT GTG ACG TTG ACA TCC GT-3′, antisense, 5′-CCT AGA AGC ATT TGC GGT GCA CGA TG-3′ for the β-actin (GenBank accession number NM_031144). The PCR products were separated by electrophoresis on an agarose gel in the presence of ethidium bromide and visualized under ultraviolet light. The molecular identity of the resultant product was confirmed by restriction analysis with two different restriction enzymes or sequence analysis using a DNA sequencer (Prism 310; Applied Biosystems).

Quantitative Real-Time PCR

Quantitative real-time PCR was performed on a sequence detection system (Prism 7700 with 2× SYBR Green PCR Master Mix; Applied Biosystems) according to the manufacturer's protocol. To quantify the amount of specific mRNA in the samples, a standard curve was generated for each run using a plasmid (pGEM-T Easy Vector; Promega, Madison, WI) containing the gene of interest. This enabled standardization of the initial mRNA content of cells relative to the amount of β-actin. The PCR was performed using rat GLUT1-, GLUT3-, SVCT2-, or β-actin–specific primers, and the cycling parameters were those given for RT-PCR analysis.

Immunostaining Analysis

Cells were cultured on a rat tail collagen-type I–coated coverslip (BD Biosciences, Lincoln Park, NJ) at 33°C for 48 hours. After removal of medium, cells were washed with PBS and fixed in 4% formaldehyde-PBS for 10 minutes at room temperature. Cells were permeated with 0.2% Triton X-100 in PBS for 15 minutes and incubated with blocking agent solution (Block Ace; Dainihon Pharmaceutical Co., Osaka, Japan) for 60 minutes. After washing with PBS, cells were further incubated with rabbit anti-GLUT1 antibody (Chemicon, Temecula, CA), rabbit anti-GLUT3 antibody (Chemicon) or goat anti-SVCT2 antibody (1:200 dilution; Santa Cruz Biotechnology, Santa Cruz, CA) as a primary antibody with 1% BSA for 3 hours at room temperature. Cells were washed with PBS and incubated for 1 hour at room temperature with FITC-conjugated anti-rabbit IgG (Chemicon) or FITC-conjugated anti-goat IgG (Chemicon) (1:50 dilution) as a secondary antibody. Cells were subsequently stained with propidium iodide and viewed by confocal laser scanning microscope (LSM 510; Carl Zeiss Meditec, Oberkochen, Germany). The control experiments were performed in parallel, with normal rabbit or goat IgG used instead of the primary antibody.

Data Analysis

The uptake of [^{14}C]DHA and [^{14}C]AA by TR-iBRB2 cells was expressed as the cell-to-medium (cell/medium) ratio

$$\text{Cell/medium ratio} = ([^{14}\text{C}]\text{ dpm per mg cell protein})/([^{14}\text{C}]\text{ dpm per }\mu\text{L medium}) \quad (5)$$

The [^{3}H]D-mannitol uptake study was performed to estimate the volume of adhering water. The resultant cell/medium ratio was 0.1 to 0.2 μL/mg protein, more than 10 times lower than that of [^{14}C]DHA. Therefore, adhering water was ignored when calculating the cell/medium ratio.

For kinetic studies, the K_m and the maximum uptake rate (J_{max}) of DHA were calculated, using the nonlinear least-squares regression analysis program, MULTI[24]

$$J = J_{max} \times [S]/(K_m + [S]) \quad (6)$$

where J and $[S]$ are the uptake rate of DHA at 1 minute and the concentration of DHA, respectively.

The 50% inhibition concentration (IC_{50}) of D-glucose for [^{14}C]DHA uptake by TR-iBRB2 cells was calculated by fitting the data to a sigmoidal inhibition model[25] using MULTI[24]

$$V = V_0/[1 + ([I]/IC_{50})^n] \quad (7)$$

where V and V_0 are the uptake of [^{14}C]DHA in the presence and absence of D-glucose, respectively, and [I] and n is the concentration of D-glucose and the Hill coefficient, respectively.

Unless otherwise indicated, all data are expressed as the mean ± SEM. Statistical significance of differences among means of several groups was determined by one-way analysis of variance (ANOVA) followed by the modified Fisher least-squares difference method.

Results

Blood-to-Retina Transport of Vitamin C across the BRB

The in vivo blood-to-retina influx transport of DHA, AA, and D-mannitol across the BRB was evaluated and compared with other tissues by means of the integration plot analysis after intravenous administration of each of the radio-labeled compounds to rats (Fig. 1). The $K_{in,\ retina}$ of [^{14}C]DHA was determined to be 2.44×10^3 μL/(min · g retina) from the slope representing the apparent influx permeability clearance across the BRB, using equation 4, whereas the $K_{in,\ retina}$ of [^{14}C]AA was 65.4 μL/(min · g retina) (Fig. 1A; Table 1). $K_{in,\ retina}$ for [^{14}C]DHA was 37.3-fold greater than that for [^{14}C]AA. A similar difference was observed in the brain: 38.1 for the ratio between the $K_{in,\ brain}$ of [^{14}C]DHA and [^{14}C]AA, whereas it was only 3.79 in the heart, which does not have a barrier between blood and organ (Figs. 1B, 1C; Table 1). In the comparison between retina and brain, the $K_{in,\ retina}$ of [^{14}C]DHA and [^{14}C]AA was approximately eight times greater than the $K_{in,\ brain}$, indicating that vitamin C transport across the BRB is greater

TABLE 1. The Apparent Influx Permeability Clearance (K_{in}) per Gram Rat Tissue and Blood/Plasma Ratio (R_B) of [^{14}C]DHA, [^{14}C]AA, and [^{3}H]D-Mannitol

Groups	$K_{in,\ retina}$ (μL/(min · g retina))	$K_{in,\ brain}$ (μL/(min · g brain))	$K_{in,\ heart}$ (μL/(min · g heart))	R_B
[^{14}C]DHA	$2.44\times10^3 \pm 0.05\times10^3$	309 ± 53	49.7 ± 15.1	0.65 ± 0.01
[^{14}C]AA	65.4 ± 10.5	8.12 ± 1.34	13.1 ± 11.0	ND
[^{3}H]D-Mannitol	ND	1.65 ± 0.38	10.8 ± 5.25	0.58 ± 0.03

K_{in} was estimated from the initial slope in Figure 1 and is expressed as the mean ± SD. R_B was determined at 3 minutes after intravenous administration of [^{14}C]DHA or [^{3}H]D-mannitol and is expressed as the mean ± SEM (n = 3). ND, not determined.

than that across the BBB. To examine whether blood cells in capillaries contribute to concentrative uptake in the retina, the apparent concentration ratio between blood and plasma (R_B) was measured. The R_B of [^{14}C]DHA were constant over 10 minutes and not much different from that of [^{3}H]D-mannitol at 3 minutes after administration (Table 1). These results support the hypothesis that the blood-to-retina DHA transport is much greater than that of AA.

Figure 2 shows the HPLC chromatograms of [^{14}C]DHA and [^{14}C]AA present in the retina and plasma after intravenous administration of 5 μCi [^{14}C]DHA. [^{14}C]DHA in plasma was rapidly changed into AA after administration and almost all the [^{14}C]DHA was converted in 5 minutes (Figs. 2E, 2F). [^{14}C]DHA accumulated in the retina as AA in a time-dependent manner (Figs. 2C, 2D).

[^{14}C]DHA and [^{14}C]AA Uptake by TR-iBRB2 Cells

To elucidate the transport mechanism of DHA, TR-iBRB2 cells were used as an in vitro rat inner BRB model.[21–23] The [^{14}C]DHA and [^{14}C]AA uptakes by TR-iBRB2 cells exhibited time-dependent increases for at least 3 minutes, with an initial uptake rate of 25.6 μL/(min · mg protein) and 0.700 μL/(min · mg protein), respectively (Fig. 3A). The uptake clearance of [^{14}C]DHA in TR-iBRB2 cells was 36.6 times greater than that of [^{14}C]AA. The [^{14}C]DHA uptake by TR-iBRB2 cells under Na^+-free conditions, using choline- or Li^+-uptake buffer, was not significantly different from the control (Na^+-uptake buffer; Fig. 3B). The [^{14}C]DHA uptake by TR-iBRB2 cells took place in a concentration-dependent manner with a K_m of 93.4 ± 18.8 μM and a J_{max} of 10.7 ± 1.2 nmol/(min · mg protein) (mean ± SD; Fig. 4), indicating that DHA is transported through an Na^+-independent carrier-mediated transport system in TR-iBRB2 cells.

Inhibitory Effect of Several Compounds on [^{14}C]DHA Uptake

The effect of glucose transporters' substrates and inhibitors on [^{14}C]DHA uptake by TR-iBRB2 cells is summarized in Table 2. D-Glucose, 3-OMG, and 2-deoxyglucose (2-DG), glucose transporters' substrates, at 30 mM, caused marked inhibition (86.4%, 81.1%, and 90.9%, respectively). L-Glucose at 30 mM caused no significant inhibition. Phloretin and cytochalasin B, glucose transporter inhibitors, at 10 μM, produced an inhibition of 60.8% and 83.4%, respectively, whereas the same concentration of phlorizin and cytochalasin E as a control for phloretin and cytochalasin B, respectively, did not have any significant effect. This inhibition of [^{14}C]DHA uptake supports the hypothesis that facilitative glucose transporters are involved in the uptake process by TR-iBRB2 cells. Moreover, [^{14}C]DHA uptake was inhibited by D-glucose in a concentration-dependent manner with an IC_{50} of 5.56 ± 0.57 mM (mean ± SD; Fig. 5).

Expression of GLUT1, GLUT3, SVCT1, and SVCT2 in TR-iBRB2 Cells

To determine vitamin C transporter expression in TR-iBRB2 cells, we performed RT-PCR analysis, using total RNA isolated

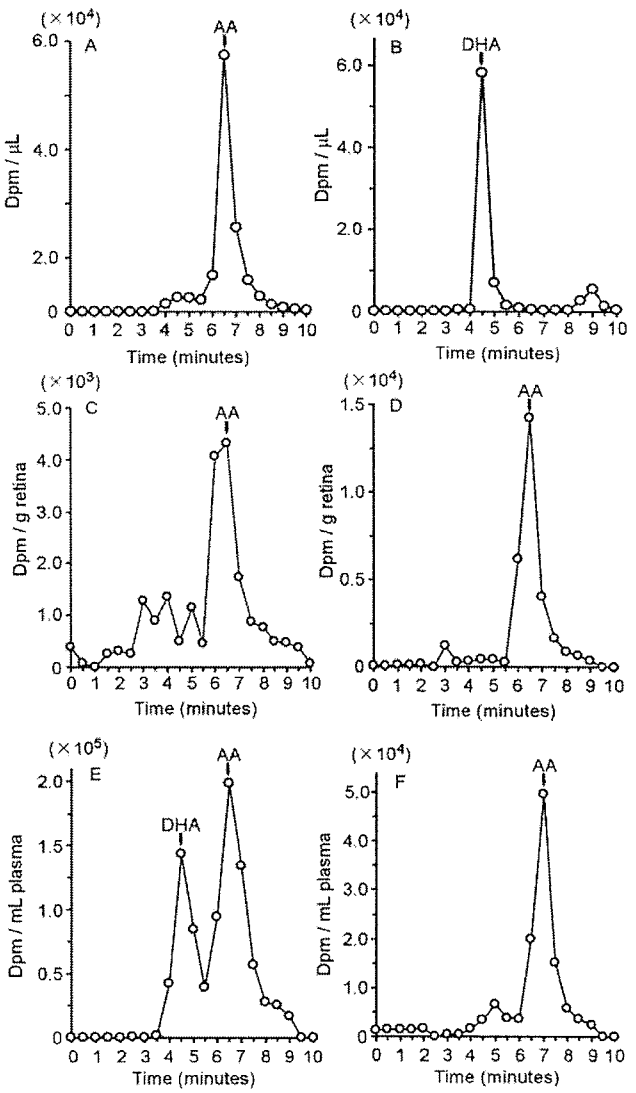

FIGURE 2. Typical HPLC chromatogram of samples of retina (**C**, **D**) and plasma (**E**, **F**) after intravenous administration of [^{14}C]DHA (**B**). [^{14}C]DHA was generated by incubating [^{14}C]AA (**A**) with ascorbate oxidase (1 U/1 mmol AA). [^{14}C]DHA (5 μCi/rat) was injected into the femoral vein, and retinas and plasma were collected at 30 seconds (**C**, **E**) and 5 minutes (**D**, **F**).

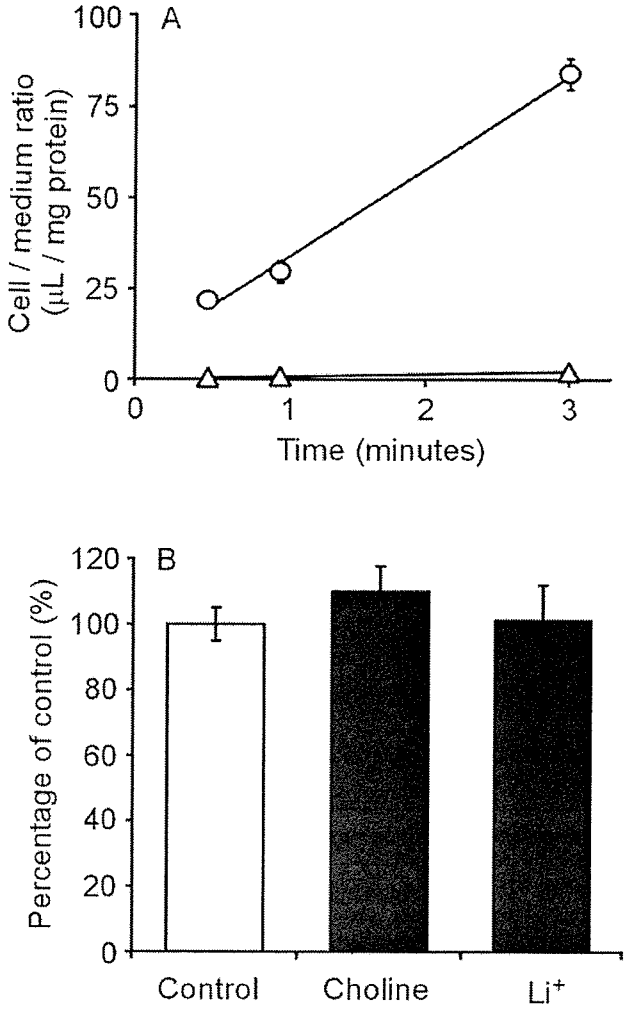

FIGURE 3. Time-course of [^{14}C]DHA and [^{14}C]AA uptake (**A**) and Na^+ independence of [^{14}C]DHA uptake by TR-iBRB2 cells (**B**). (**A**) [^{14}C]DHA (○, 0.2 μCi) and [^{14}C]AA (△, 0.2 μCi) uptake were performed at 37°C. (**B**) [^{14}C]DHA (0.2 μCi) uptake was performed in the presence or absence of Na^+ (Na^+ was replaced with equimolar choline or Li^+) at 1 minute and at 37°C. The uptake was expressed as the cell/medium ratio according to equation 5. Each point represents the mean ± SEM (n = 4).

from TR-iBRB2 cells, brain, and kidney and specific primers of rat GLUT1 and -3 and rat SVCT1 and -2 (Fig. 6A). β-Actin was used as a housekeeping gene. GLUT1, GLUT3, and SVCT2 mRNA were amplified at 503, 398, and 358 bp, respectively, in TR-iBRB2 cells and brain, whereas SVCT1 mRNA was not. The mRNA expression levels of GLUT1, GLUT3, and SVCT2 were determined in TR-iBRB2 cells by quantitative real-time PCR analysis. The quantity of expression mRNA, compensated with β-actin, for GLUT1, GLUT3, and SVCT2 was $7.39 \times 10^{-3} \pm 0.91 \times 10^{-3}$, $1.98 \times 10^{-4} \pm 0.25 \times 10^{-4}$, and $1.84 \times 10^{-5} \pm 0.26 \times 10^{-5}$, respectively (Fig. 6B). Accordingly, the expression of GLUT1 mRNA was 37.3 and 402 times greater, respectively, than that of GLUT3 and SVCT2 mRNA in TR-iBRB2 cells.

The expression and localization of GLUT1, GLUT3, and SVCT2 protein in TR-iBRB2 cells were examined by confocal laser scanning microscope (Fig. 7). The immunostaining by anti-GLUT1 (Figs. 7A, 7D) and anti-GLUT3 antibody (Figs. 7B, 7E) was observed in TR-iBRB2 cells. No significant fluorescence was observed in TR-iBRB2 cells stained with anti-SVCT2

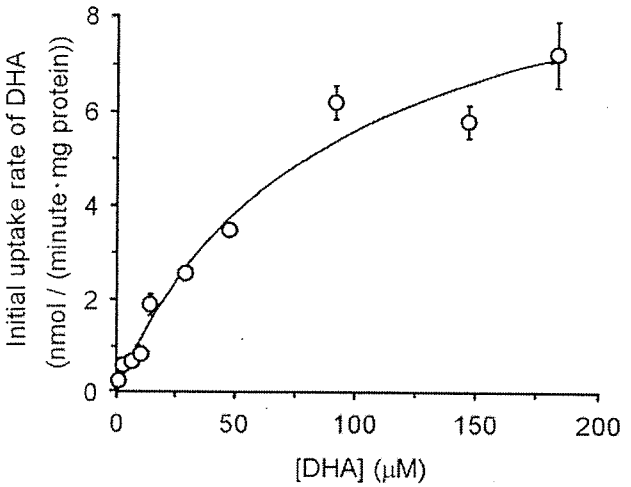

FIGURE 4. Concentration-dependence of DHA uptake by TR-iBRB2 cells. [^{14}C]DHA uptake was performed at 2 minutes at 37°C, over the concentration range from 1.7 μM (4.9 nCi) to 180 μM (4.4 μCi). Data are the mean ± SEM (n = 4). The K_m and J_{max} were 93.4 ± 18.8 μM and 10.7 ± 1.2 nmol/(min · mg protein), respectively (mean ± SD).

antibody (Figs. 7C, 7F) and normal IgG (data not shown). An x-z section in GLUT1 and GLUT3 staining (Figs. 7D, 7E) showed that fluorescence (green) was located over the cell nucleus (red), providing supporting evidence that GLUT1 and GLUT3 are mainly localized on the cell surface of TR-iBRB2 cells.

DISCUSSION

The present study produces, for the first time, in vivo evidence that vitamin C is mainly transported as DHA across the BRB and accumulates as AA in the retina (Figs. 1 and 2). DHA is transported by a facilitative glucose transporter, most likely GLUT1, which is expressed at the luminal (blood) and abluminal (retina) side of the inner BRB and RPE (outer BRB),[17] although the additional contribution of GLUT3 cannot be ruled out at the present time.[26] GLUT1 mRNA expression in TR-iBRB2 cells used as an in vitro model of inner BRB was 37 times greater than that of GLUT3. Nevertheless, GLUT1 and -3 proteins were substantially expressed on the cell surface of TR-iBRB2 cells (Figs. 6, 7). [^{14}C]DHA uptake by TR-iBRB2 cells took place in an Na^+-independent and concentration-dependent manner, with a K_m of 93.4 μM (Figs. 3B, 4). This K_m is similar to that

TABLE 2. Inhibitory Effect of Several Compounds on [^{14}C]DHA Uptake by TR-iBRB2 Cells

Inhibitors	Percentage of Control
Control	100 ± 12
30 mM D-Glucose	13.6 ± 3.1*
30 mM L-Glucose	81.3 ± 2.7
30 mM 3-OMG	18.9 ± 1.3*
30 mM 2-DG	9.10 ± 1.8*
10 μM Phloretin	39.2 ± 8.3*
10 μM Phloridzin	91.7 ± 8.9
10 μM Cytochalasin B	16.6 ± 7.5*
10 μM Cytochalasin E	100.3 ± 4.6

[^{14}C]DHA uptake was performed for 2 minutes at 37°C in the presence or absence of inhibitors. Data are expressed as the mean ± SEM (n = 4–12). 3-OMG: 3-O-methyl-D-glucose, 2-DG: 2-deoxyglucose.

* $P < 0.01$, significantly different from control.

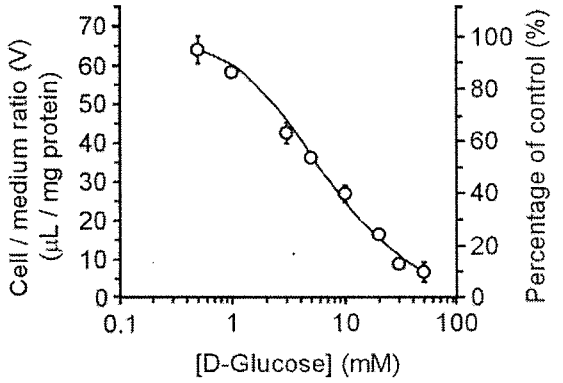

FIGURE 5. Inhibitory effect of D-glucose on [^{14}C]DHA uptake by TR-iBRB2 cells. [^{14}C]DHA uptake was performed in the presence (0.5–50 mM) or absence (control) of D-glucose at 2 minutes and at 37°C. Each point represents the mean ± SEM (n = 4). The IC_{50} is 5.56 ± 0.57 mM (mean ± SD).

obtained for DHA uptake (K_m = 60 μM) in *Xenopus* oocytes expressing GLUT1.[12] Moreover, [^{14}C]DHA uptake by TR-iBRB2 cells was strongly inhibited by glucose transporter substrates, such as D-glucose, 3-OMG, and 2-DG and inhibitors, such as phloretin and cytochalasin B (Table 2).[27]

The $K_{in,\ retina}$ of [^{14}C]DHA (2.44 × 10^3 μL/(min · g retina)) was 37 times greater than that of [^{14}C]AA (65.4 μL/(min · g retina); Fig. 1A). This result agrees with the ratio between [^{14}C]DHA and [^{14}C]AA uptake clearance in TR-iBRB2 cells (Fig. 3A) and supports the hypothesis that DHA is predominantly transported through facilitative glucose transporters at the BRB rather than by AA. However, AA transport into the retina cannot be fully ruled out at the present time, because the $K_{in,\ retina}$ of [^{14}C]AA was significantly greater than that of [^{3}H]D-mannitol, which was used as a nonpermeable paracellular marker (Fig. 1A). In addition, an Na^+-dependent AA transport process seems to be present in the bovine RPE.[10] In the brain, a similar difference in the $K_{in,\ brain}$ between [^{14}C]DHA and [^{14}C]AA supports the hypothesis that glucose transporters at the blood–organ barriers such as the BRB and BBB facilitate transport of DHA, but not of AA, as reported at the BBB,[16] since, in the heart, there was not a great difference in the $K_{in,\ heart}$ between [^{14}C]DHA and [^{14}C]AA (Table 1). The $K_{in,\ retina}$ of [^{14}C]DHA and [^{14}C]AA was approximately eight times greater than the corresponding values in brain (Table 1). Possible reasons for this are that the amounts of retinal and brain capillary endothelial cells represent a small percentage of the weight of the entire retina and 0.1% to 0.2% of the weight of the entire brain, respectively,[28,29] and RPE (outer BRB) contributes to the supply of essential molecules in the outer segment of the retina, whereas choroid plexus epithelial cells (blood–cerebrospinal fluid barrier) do not play a major role in supplying them for the entire brain.[7,30] Moreover, Root-Bernstein et al.[31] reported the evidence that DHA, rather than AA, is taken up by human RPE, and its uptake is inhibited by D-glucose in a concentration-dependent manner.[31] GLUT1 expression in rat retinal capillary endothelial cells is greater than that in rat brain capillary endothelial cells.[32,33]

The innate vitamin C regulatory mechanism in the retina most likely involves GLUT1 supplying DHA to the retina at the luminal and abluminal sides of the inner BRB and RPE (outer BRB), and the transported DHA is reduced to AA and accumulates in the retina as an antioxidant. Even though GLUT1 is not a concentrative transporter, DHA is rapidly reduced to AA and thus is trapped within the retina (Fig. 2). The conversion of [^{14}C]DHA to [^{14}C]AA in plasma is very rapid compared with the initial uptake of [^{14}C]DHA (Figs. 1, 2). The level of [^{14}C]DHA remaining in plasma seems to be underestimated, because it cannot be ignored that [^{14}C]DHA converts to [^{14}C]AA during manipulation of the assay.[34] Notably, blood-to-retina influx transport of [^{14}C]DHA takes place, since it was much greater than that of [^{14}C]AA (Fig. 1, Table 1). Although the affinity of DHA for facilitative glucose transporters (K_m = 93.4 μM, Fig, 4) is greater than that of D-glucose, (the K_m estimated for D-glucose uptake by the retina across the rat BRB was 7.81 mM),[35] DHA uptake through facilitative glucose transporters is competitively inhibited by D-glucose, and the normal plasma D-glucose concentration in most mammals is approximately 5 mM. D-Glucose inhibited [^{14}C]DHA uptake by TR-

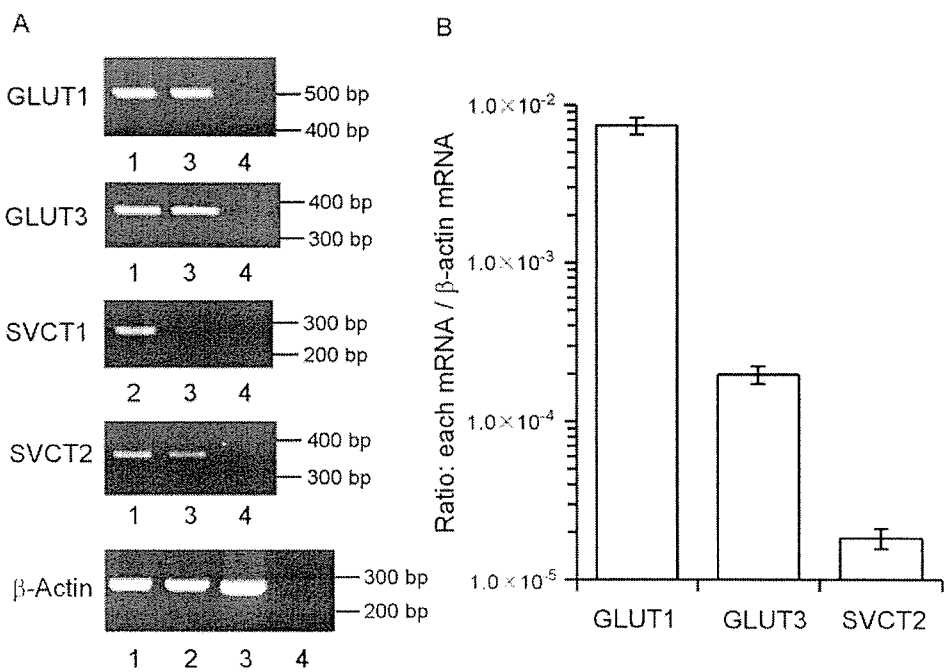

FIGURE 6. RT-PCR analysis of GLUT1, GLUT3, SVCT1, SVCT2, and β-actin (**A**) and the amount of GLUT1, GLUT3, and SVCT2 mRNA (**B**) in TR-iBRB2 cells. (**A**) *Lane 1*: rat brain; *lane 2*: rat kidney; *lane 3*: TR-iBRB2 cells; *lane 4*: in the absence of reverse transcriptase for TR-iBRB2 cells. Rat brain was used as a positive control for GLUT1, GLUT3, and SVCT2, and rat kidney was used as a positive control for SVCT1. (**B**) The amount of GLUT1, GLUT3, and SVCT2 mRNA in TR-iBRB2 cells was determined by quantitative real-time PCR analysis. Data are the mean ± SEM (n = 4). The GLUT1, GLUT3, and SVCT2 mRNA content relative to β-actin mRNA (GLUT1/β-actin, GLUT3/β-actin, and SVCT2/β-actin) was 7.39 × 10^{-3} ± 0.91 × 10^{-3}, 1.98 × 10^{-4} ± 0.25 × 10^{-4}, and 1.84 × 10^{-5} ± 0.26 × 10^{-5}, respectively.

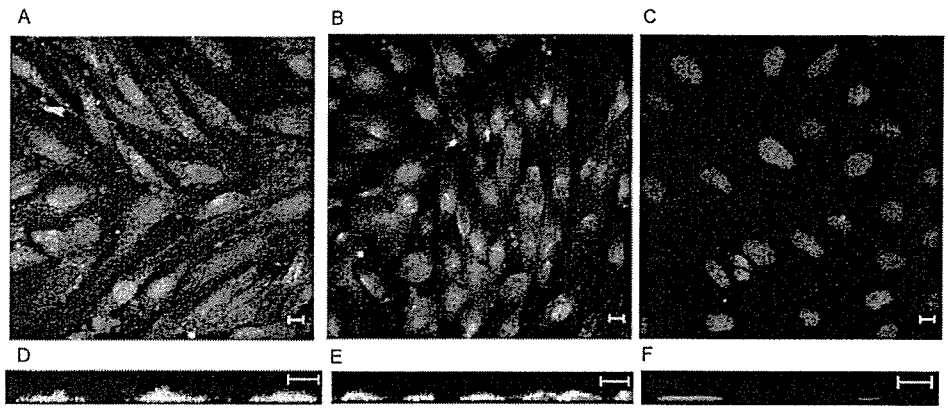

FIGURE 7. Immunostaining analysis of GLUT1, GLUT3, and SVCT2 in TR-iBRB2 cells. TR-iBRB2 cells were immunostained by anti-GLUT1 (**A**, **D**), anti-GLUT3 (**B**, **E**), and anti-SVCT2 (**C**, **F**) antibodies. (**A**, **B**, **C**) *x-y* sections; (**D**, **E**, **F**) *x-z* sections. *Green*: immunoreactivity by each antibody; *red*: nuclei stained by propidium iodide. Scale bar, 10 μm.

iBRB2 cells, with an IC_{50} of 5.56 mM (Fig. 5). Therefore, DHA transport by facilitative glucose transporters across the BRB does not exhibit complete inhibition (i.e., approximately 50%), under normal conditions. The DHA plasma concentration has been recently determined to be approximately 10 μM (10%–20% of total plasma ascorbate concentration) in the rat and human.[14,15] Moreover, DHA is produced by metal-binding proteins, such as serum albumin and by superoxide anions in endothelial cells.[36,37] However, hyperglycemia (i.e., diabetic mellitus) increases the blood D-glucose concentration to 20 mM or higher, leading to the inhibition of DHA transport at the BRB.[31] Indeed, [^{14}C]DHA uptake by TR-iBRB2 cells was inhibited by 79% at a concentration of 20 mM D-glucose (Fig. 5). Although there is contradictory evidence showing regulation of GLUT1 expression in retinal capillary endothelial cells under diabetic conditions,[33,38] rats with streptozotocin-induced diabetes show downregulation of GLUT1 expression by 50% in the retina.[33] In light of these findings, diabetic patients may experience enhanced oxidative stress in the retina because of reduced influx of DHA, leading to the hypothesis that diabetic retinopathy involves dysfunction of DHA influx at the BRB.

From a pharmacological viewpoint, intravenous administration of DHA may be effective for retinal ischemia-reperfusion to protect the neural retina against oxidative stress. Huang et al.[39] reported that intravenous administration of DHA mediates cerebroprotection after reperfused and nonreperfused cerebral ischemia, but this did not happen with AA. This suggests that DHA can use a transportable prodrug of AA across the BRB and BBB to exert its neuroprotective effects. However, DHA has membrane-disruptive effects in erythrocytes and renal brush border membrane and may destroy the pancreatic beta cells.[40,41] Further studies are needed to elucidate the relationship between pharmacologically effective and toxicologically adverse concentrations of DHA in plasma.

In conclusion, vitamin C is predominantly transported as DHA through facilitative glucose transporters at the BRB and accumulates as AA in the retina. The physiological role of facilitative glucose transporters at the BRB appears to involve the supply of vitamin C from the circulating blood to the retina to protect the neural retina against oxidative stress. These findings provide important information to help us understand the physiological and pathophysiological roles of facilitative glucose transporters at the BRB and assist in the design of a suitable DHA dosage regimen for pharmacological therapies.

Acknowledgments

The authors thank Hisashi Iizasa and Masanori Tachikawa for valuable discussion.

References

1. Friedman PA, Zeidel ML. Victory at C. *Nat Med.* 1999;5:620–621.
2. Ham WT Jr, Mueller HA, Ruffolo JJ Jr, et al. Basic mechanisms underlying the production of photochemical lesions in the mammalian retina. *Curr Eye Res.* 1984;3:165–174.
3. Woodford BJ, Tso MOM, Lam KW. Reduced and oxidized ascorbates in guinea pig retina under normal and light-exposed conditions. *Invest Ophthalmol Vis Sci.* 1983;24:862–867.
4. Nielsen JC, Naash MI, Anderson RE. The regional distribution of vitamin E and C in mature and premature human retinas. *Invest Ophthalmol Vis Sci.* 1988;29:22–26.
5. Greco AM, Fioretti F, Rimo A. Relationship between hemorrhagic ocular disease and vitamin C deficiency: clinical and experimental data. *Acta Vitaminol Enzymol.* 1980;2:21–25.
6. Kowluru RA, Tang J, Kern TS. Abnormalities of retinal metabolism in diabetes and experimental galactosemia. *Diabetes.* 2001;50:1938–1942.
7. Cunha-Vaz JG. The blood-retinal barriers. *Doc Ophthalmol.* 1976;41:287–327.
8. Stewart PA, Tuor UI. Blood-eye barriers in the rat: correlation of ultrastructure with function. *J Comp Neurol.* 1994;340:566–576.
9. Tsukagoshi H, Tokui T, Mackenzie B, et al. A family of mammalian Na^+-dependent L-ascorbic acid transporters. *Nature.* 1999;399:70–75.
10. Khatami M. Na^+-linked active transport of ascorbate into cultured bovine retinal pigment epithelial cells: heterologous inhibition by glucose. *Membr Biochem.* 1987–1988;7:115–130.
11. Kannan R, Stolz A, Ji Q, Prasad PD, Ganapathy V. Vitamin C transport in human lens epithelial cells: evidence for the presence of SVCT2. *Exp Eye Res.* 2001;73:159–165.
12. Vera JC, Rivas CI, Fischbarg J, Golde DW. Mammalian facilitative hexose transporters mediate the transport of dehydroascorbic acid. *Nature.* 1993;364:79–82.
13. Rumsey SC, Kwon O, Xu GW, Burant CF, Simpson I, Levine M. Glucose transporter isoforms GLUT1 and GLUT3 transport dehydroascorbic acid. *J Biol Chem.* 1997;272:18982–18989.
14. Koshiishi I, Imanari T. Quantification of carbamylated dehydroascorbate derivative produced from cyanate and dehydroascorbate. *J Chromatogr B.* 1998;709:150–156.
15. Nakayama H, Akiyama S, Inagaki M, Gotoh Y, Oguchi K. Dehydroascorbic acid and oxidative stress in haemodialysis patients. *Nephrol Dial Transplant.* 2001;16:574–579.
16. Agus DB, Gambhir SS, Pardridge WM, et al. Vitamin C cross the blood-brain barrier in the oxidized form through the glucose transporters. *J Clin Invest.* 1997;100:2842–2848.
17. Takata K, Kasahara T, Kasahara M, Ezaki O, Hirano H. Ultracytochemical localization of the erythrocyte/HepG2-type glucose transporter (GLUT1) in cells of the blood-retinal barrier in the rat. *Invest Ophthalmol Vis Sci.* 1992;33:377–383.
18. Kumagai AK, Glasgow BJ, Pardridge WM. GLUT1 glucose transporter expression in the diabetic and nondiabetic human eye. *Invest Ophthalmol Vis Sci.* 1994;35:2887–2894.